EPR evidence of extrinsic symmetry-breaking defects in nominally pure $KTaO_3$

A. P. Pechenyi and M. D. Glinchuk
Institute for Material Sciences, Academy of Sciences of Ukraine, 252180 Kiev, Ukraine

C. B. Azzoni and F. Scardina
Department of Physics, "Alessandro Volta," Università degli Studi di Pavia, via A. Bassi 6, I-27100 Pavia, Italy

A. Paleari
Department of Physics, Università degli Studi di Milano, via Celoria 16, I-20133 Milano, Italy
(Received 31 May 1994)

EPR measurements on nominally pure (undoped) $KTaO_3$ single crystals at low temperature (4.2 K) are reported. Evidence is brought of impurity defects analyzed through the experimental spin-Hamiltonian parameters. Axial EPR spectra of Fe^{3+} in different cation positions are detected. An orthorhombic spectrum is found and attributed to Fe^{3+} substituting for K^+ ions and involving nearby potassium vacancies as charge compensators. Manganese impurities are also observed following illumination of the sample to cause a change of the Mn valence state.

I. INTRODUCTION

Phase transitions induced by dipole impurities in highly polarizable crystals are the subject of steadfast attention in recent years. One of the most investigated materials is the incipient ferroelectric $KTaO_3$. Its cubic perovskite phase is stabilized down to low temperature.[1] The cubic symmetry is broken down in mixed crystals $K_{1-x}Li_xTaO_3$ (KTLi), $K_{1-x}Na_xTaO_3$ (KTNa), and $KTa_{1-x}Nb_xO_3$ (KTNb) owing to dipole interaction of off-center Li^+, Nb^{5+}, and apparently Na^+ ions.[2] In these compounds the behavior of the polar state below the transition temperature T_c is very complex. Both the ferroelectric[3] and dipole glass state[4] have been invoked. Some low-temperature features have been discussed in terms of "quadrupole glass,"[5] "cooperative dipole glass,"[6] or "displacive ferroelectric order-disorder-like transition."[7] Whatever model is used to explain this low-temperature polar state, symmetry-breaking (SB) defects yielding random electric and elastic fields[8] should be taken into account. The local dipole moments of SB defects may polarize adjacent unit cells giving rise to ferroelectric microregions.

There are indeed several indirect indications of SB defects in $KTaO_3$ mixed compounds, as defect-induced first-order Raman scattering[9–11] and second harmonic (hyper-Rayleigh) light scattering.[12] SB defects were also proposed to exist in nominally pure $KTaO_3$, as suggested by near-infrared fluorescence spectra at low temperatures[11,13] and photoluminescence[14] measurements. Moreover, the light induced photocurrent in $KTaO_3$,[15] as well as in KTLi,[16] is supposed to be connected with defect-related photocarriers.[17]

It should be noted that, despite all the reported experimental evidence, there are different opinions and no direct indication about the nature of the SB defects. It was suggested that the relevant defects in $KTaO_3$ are intrinsic,[11,14] whereas other workers proposed an important role of unknown impurities.[10,12,17] So, the direct identification of these defects is of great importance in understanding their role on the phase transitions.

In this paper we report the results of EPR measurements on nominally pure (undoped) $KTaO_3$ single crystals, and present evidence of the extrinsic nature of the main defects. The investigations have been carried out at low-temperature (4.2 K) to reveal weak EPR signals from small amounts (less than a few ppm) of paramagnetic impurities. Light illumination of the samples allowed us to observe otherwise nonparamagnetic centers by changing their valence state.

II. EXPERIMENTAL DETAILS

Two $KTaO_3$ single crystals have been studied: sample 1, grown by spontaneous crystallization technique, is an optically transparent and colorless sample. Sample 2, grown by Czochralski method, has a slightly yellow color. The starting components are 99.99% pure Ta_2O_5 and 99.999% pure K_2CO_3 with the excess of the latter. The samples have lamellar form, the crystalline (100) plane of cubic lattice being parallel to the main surfaces.

EPR measurements have been performed using a low-power X band EPR spectrometer (9.45 GHz) with an Oxford system for low-temperature experiments. The spectra have been taken at 4.2 K. Refinement of the orientation of the samples in the magnetic field **B** has been achieved by minimizing the multiplicity of the signals arising from known axial defects with an accuracy better than 0.2°. Sample illumination experiments have been performed with a 200 W short arc Hg lamp.

III. RESULTS

Both of the $KTaO_3$ samples show well defined EPR signals at 4.2 K. In total, we have identified four signals

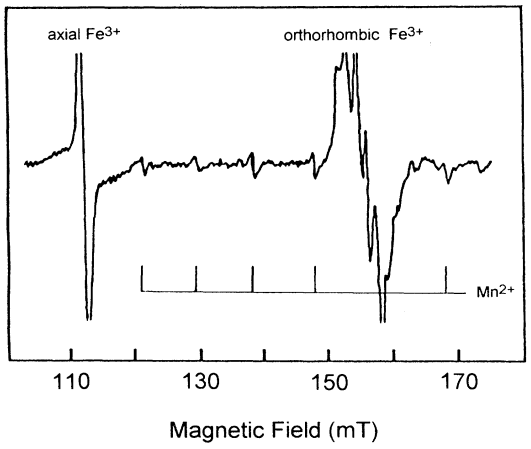

FIG. 1. EPR spectrum ($\nu=9.45$ GHz) of nominally pure $KTaO_3$ (sample 2) at 4.2 K, with $B\|[100]$. Axial Fe^{3+} lines (the broader line appears as wings at the sides of the strong narrower line) are indicated together with the orthorhombic Fe^{3+} lines and the six resonance lines of the hyperfine structure of the $(-5/2\leftrightarrow-3/2)_1$ transition of the light-induced Mn^{2+} spectrum (see also Table I).

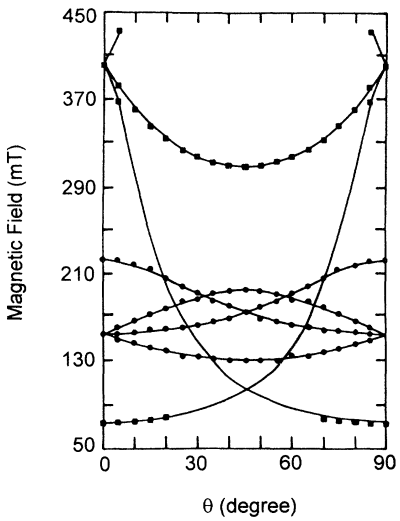

FIG. 2. Angular dependence of the orthorhombic Fe^{3+} EPR spectrum (sample 2) in the (001) plane at 4.2 K. ● and ■ denote transitions between $\pm3/2$ and $\pm1/2$ Kramers doublets, respectively. The solid lines are obtained from the best-fitting computer calculation.

with local symmetry lower than cubic: two axial, an orthorhombic one, and a signal induced by Hg-lamp irradiation (Fig. 1). Only an axial signal has been detected in the sample 1, whilst we have observed both of the axial signals and the orthorhombic one in the sample 2; see Fig. 1. Illumination of the samples causes no detectable change of the preexistent signals but does produce the appearance of another signal in sample 2 only. In the following sections we report the details of the features of the EPR signals.

A. Axial signals

We have observed two kinds of axial spectra with the same angular dependence on the magnetic-field direction but of very different linewidths (a few tenths of mT against several mT). They consist of three lines, one with $g\simeq6$ and the others with a strong angular dependence when **B** is rotated in a (001) plane. The narrow spectrum, the only one observed in sample 1, is an order of magnitude less intense than in sample 2. The angular dependence in the (001) plane indicates that the defect axis is along the ⟨100⟩ directions. Both of these axial signals can be attributed to Fe^{3+} ions as discussed afterwards.

B. Orthorhombic signal

In sample 2 we have also observed an orthorhombic signal whose angular dependence at $T=4.2$ K for **B** in the (001) plane is shown in Fig. 2. Its anisotropy and multiplicity indicate that the z axis of the responsible defect is along any of the ⟨110⟩ crystal directions. Computer calculation of the crystal-field parameters has been achieved by fitting the measured angular dependence of the spectrum with the spin Hamiltonian of orthorhombic symmetry in the form[18]

$$H=\beta(g_xB_xS_x+g_yB_yS_y+g_zb_zS_z)+\tfrac{1}{3}(b_2^0O_2^0+b_2^2O_2^2)+\tfrac{1}{60}(b_4^0O_4^0+b_4^2O_4^2+b_4^4O_4^4)\,.$$

The obtained values are the following: $g_x=1.990$, $g_y=1.996$, $g_z=1.998$, $b_2^0=D=0.474$ cm^{-1}, $b_2^2=3E=0.276$ cm^{-1}, $b_4^0=-2\times10^{-4}$ cm^{-1}, $b_4^2=2.1\times10^{-4}$ cm^{-1}, and $b_4^4=1.1\times10^{-2}$ cm^{-1} with the z axis along [110] directions.[19] The calculated angular dependences are plotted in Fig. 2. The crystal-field parameters are temperature dependent and E/D decreases with increasing the temperature.

C. Light-induced signal

After a few minutes of continuous Hg-lamp illumination of the sample 2 at 4.2 K we have observed an EPR spectrum. The light-induced EPR centers prove to be very stable. The heating of the sample up to room temperature does not lead to any change of the spectrum after recooling at 4.2 K. The spectrum disappeared completely only after several hours at room temperature. We have not observed any noticeable changes of the axial and orthorhombic EPR spectra during illumination and heat treatment of the sample 2.

When the magnetic field is along a ⟨100⟩ crystal axis the spectrum consists of several sextets of lines in a wide magnetic-field range. The typical structure due to the hyperfine interaction with a nuclear spin $I=5/2$ allows us undoubtedly to assign the light-induced spectrum to Mn^{2+} paramagnetic centers ($S=5/2$, $I=5/2$). The line positions arising from parallel and perpendicular defect orientations are well reproduced (see Table I) by the fol-

TABLE I. Experimental and calculated resonance fields B_r for axial Mn^{2+} EPR spectrum with $B\|[100]$. Parameters of calculation are presented in the text.

B_r experimental (mT)	B_r calculated (mT)	Transition
121.9	121.75	$(-5/2\leftrightarrow-3/2)_\perp$
130.2	130.16	$(-5/2\leftrightarrow-3/2)_\perp$
138.8	138.92	$(-5/2\leftrightarrow-3/2)_\perp$
148.0	148.03	$(-5/2\leftrightarrow-3/2)_\perp$
[a]	153.11	$(-3/2\leftrightarrow-1/2)_\perp$
[a]	157.48	$(-5/2\leftrightarrow-3/2)_\perp$
162.7	162.79	$(-3/2\leftrightarrow-1/2)_\perp$
167.2	167.24	$(-5/2\leftrightarrow-3/2)_\perp$
172.2	172.43	$(-3/2\leftrightarrow-1/2)_\perp$
181.5	181.93	$(-3/2\leftrightarrow-1/2)_\perp$
191.2	191.35	$(-3/2\leftrightarrow-1/2)_\perp$
199.3	199.94	$(-3/2\leftrightarrow-1/2)_\perp$
286.9	286.50	$(-1/2\leftrightarrow1/2)_\perp$
294.8	295.13	mixed
303.2	302.10, 304.37	mixed
311.7	311.32	$(-1/2\leftrightarrow1/2)_\perp$
313.5	313.34	mixed
320.9	320.55	$(-1/2\leftrightarrow1/2)_\perp$
329.7	329.52	mixed
330.5	330.09	$(-1/2\leftrightarrow1/2)_\perp$
[a]	332.83	$(-1/2\leftrightarrow1/2)_\|$
345.8	345.39	$(-1/2\leftrightarrow1/2)_\|$
356.0	355.93	$(-1/2\leftrightarrow1/2)_\|$
358.7	359.26	mixed
364.0	364.21	$(-1/2\leftrightarrow1/2)_\|$
[b]	369.84	$(-1/2\leftrightarrow1/2)_\|$

[a]Resonance line coincides with that of rhombic or axial Fe^{3+} center.
[b]Resonance line is not observed.

lowing parameters: $g_\|=1.9978$, $g_\perp=2.0004$, $b_2^0=0.153$ cm^{-1}, $b_4^0=-1.2\times10^{-4}$ cm^{-1}, $b_4^4=2\times10^{-4}$ cm^{-1}, $^{55}A_\|=-85.9\times10^{-4}$ cm^{-1}, and $^{55}A_\perp=-82.7\times10^{-4}$ cm^{-1}. All these values correspond to those previously determined at 77 K in K band (20 GHz) (Ref. 19) with the exception of the b_2^0 value which changes from 0.148 to 0.153 cm^{-1} owing to its temperature dependence.[20]

IV. DISCUSSION

This work has been undertaken to determine the nature of the paramagnetic defects in undoped potassium tantalate. We have succeeded in revealing impurities that may be identified as the SB defects supposed to exist in $KTaO_3$.

The axial spectra constitute indeed clear evidence of the presence of iron impurities in axial sites. In fact, they correspond to the EPR spectra of axial Fe^{3+} (spin $S=5/2$) observed in iron doped $KTaO_3$. It is known[21,22] that the doping of $KTaO_3$ by iron ions induces two types of axial centers arising from Fe^{3+} ions substituting for Ta^{5+} or K^+ ions, with nearest-neighbor charge compensation (oxygen vacancy V_0 or interstitial O^{2-}, respectively). Because of the large value of the crystal-field parameter D (b_2^0) ($D=1.44$ cm^{-1} for Fe^{3+}-V_0 and $D=4.46$ cm^{-1} for Fe^{3+}-O^{2-}), the axial Fe^{3+} spectrum in X band consists of three resonance lines arising from the transition within the $\mp1/2$ Kramers doublet ($S_{eff}=1/2$, $g_{\|eff}=2$, $g_{\perp eff}=6$) from each one of the possible defect orientations along [100], [010], and [001] directions. The EPR line positions of the two variants of Fe^{3+} axial center coincide in the X band range but their linewidths are different (less than 1 mT for Fe^{3+}-O^{2-} center in K^+ site and about 5 mT for Fe^{3+}-V_0 center in Ta^{5+} site at 4.2 K). All these features are observed in the sample 2; see Fig. 1. On the other hand, the sample 1 shows only one weak axial spectrum (arising from a few ppm of iron impurities) which can be identified from its narrow linewidth as due to axial Fe^{3+} centers in K^+ positions.

We suggest that the orthorhombic spectrum also arises from Fe^{3+} ions at K^+ sites. Both the angular dependence and the range of g values show several similarities with another orthorhombic spectrum previously analyzed[19] and attributed to Fe^{3+} ions substituting for Ta^{5+} with a nearby interstitial bivalent positive ion for charge compensation in the $\langle110\rangle$ direction. But, two features discriminate our orthorhombic spectrum from the previously observed one: (i) the angular dependence of the line positions clearly deviates from the reported one, pointing to different crystal-field parameters for this center and (ii) we observe a superhyperfine structure of the line with $g_{eff}\approx4.3$ when $\mathbf{B}\|[100]$. These features suggest that the observed spectrum can be considered as arising from another orthorhombic Fe^{3+} center located in a different site of the host. Similarly, Fe^{3+} ions in axial sites give rise to two variants of EPR signals in doped $KTaO_3$ arising from Fe^{3+} ions substituting for Ta^{5+} or K^+. This fact leads us to suggest that the spectrum is due to Fe^{3+} in orthorhombic K^+ sites. In this case a narrower linewidth is expected than that of the other orthorhombic spectrum, as it happens for the two variants of axial Fe^{3+} signals. Really, we have observed such a difference that is just the cause of our success in resolving the superhyperfine structure at $g\simeq4.3$. In fact, the temperature-independent linewidth of the orthorhombic signal arising from Fe^{3+} substituting for Ta^{5+} was proposed to be determined by unresolved superhyperfine interaction with nearby nuclei. As regards the temperature dependence of the crystal-field parameters, the orthorhombic Fe^{3+} defect shows a behavior similar to that of the axial Fe^{3+} center in K^+ sites,[22] whereas Fe^{3+} occupying Ta^{5+} positions is characterized by temperature-independent parameters.[19,22] Following these correspondences, we tentatively attribute the signal to Fe^{3+} in K^+ orthorhombic sites. But Fe^{3+} ions substituting for K^+ ions introduce an excess of positive charge and call for a charge compensation. Hence the suggested model is a Fe^{3+} ion in K^+ site with nearby potassium vacancies V_K for charge compensation: since the orthorhombic z axis is along the $\langle110\rangle$ directions, one can expect that charge compensation occurs by either a next-nearest-neighbor potassium vacancy V_K in [110] direction or by two nearest-neighbors V_K in [100] and [010] directions.

This type of charge compensation should also be taken into account for the axial Fe^{3+} center in K^+ site. In fact, a model with a nearest-neighbor potassium vacancy in a

⟨100⟩ direction for charge compensation (Fe^{3+}-V_K center) can be regarded as an alternative model to the Fe^{3+}-O^{2-} attribution previously suggested for this center[22] and apparently supported by the observed increase of the EPR spectrum under sample treatment in oxygen atmosphere;[23] actually, the increase could be caused by an oxidation-induced shift of the Fermi level with change of the valence state of the impurities.

We remark that the iron defects responsible for the reported EPR signals are SB defects: owing for their dipole moment, they can induce polarization clusters. So, iron impurities in $KTaO_3$ must be considered in interpreting the optical properties.[24] In particular, the assumption that the enhanced luminescence in reduced samples is caused by oxygen vacancies[10,12] may have an alternative explanation connected with the change of the valence state of iron ions possibly involved in the optical emission process.

It is noteworthy that all these types of defects involve K^+ sites, as substituted cationic sites or vacancy sites for charge compensation, in both the investigated samples. Really, the presence of K^+ vacancies in the host is also important for discussing the nature of the axial Mn^{2+} center observed in this work after illumination.

There are different points of view about the model of the Mn^{2+} center. In an early work, Hannon[20] suggested that the Mn^{2+} ion was substitutional for a Ta^{5+} ion with an adjacent oxygen vacancy, and it was argued[27] that the observed motional narrowing of axial Mn^{2+} EPR lines at high temperatures arose from hopping of an oxygen vacancy between inequivalent sites. However, it was shown[28] that EPR results could be described by considering an off-center position of Mn^{2+} on K^+ site. An analysis of the Mn^{2+} hyperfine constant in $KTaO_3$,[29] as well as the value of activation energy of the hopping process,[26] showed that Mn^{2+} ions should be located on K^+ site with K^+ vacancy nearby, and the hopping process should be connected with equivalent Mn^{2+} off-center positions. Taking into account that the observed Fe^{3+} centers call for K^+ vacancies in the host, the supposed existence of Mn^{2+}-V_K centers in $KTaO_3$ becomes now more reliable.

Whereas the $KTaO_3$ crystals doped with Mn ions the Mn^{2+} EPR spectrum is observed without any light excitation,[20,25,26] in our sample the presence of Fe^{3+} ions probably forces the Mn ions into the trivalent valence state (EPR inactive because of a too short spin lattice relaxation time[26]), as in $KTaO_3$ crystals codoped with titanium and manganese.[20] The stability of these centers after illumination can be explained by hole trapping in iron of other nonparamagnetic impurities, but the question is still open: in fact, we have not observed any light-induced change of the Fe^{3+} EPR spectra, but the Mn spectrum is weak and the possible effects of its intensity changes on the Fe^{3+} signals are expected to be beyond the experimental accuracy.

V. CONCLUSIONS

Low-temperature EPR investigations of nominally pure $KTaO_3$ single crystals show that iron (in concentration of a few ppm) is present as the main impurity. Fe^{3+} ions constitute SB defects as indicated by the local symmetry reduction. All these defects involve cationic substitution, where the charge compensation is achieved through K^+ vacancies or O^{2-} ions.

A previously unobserved orthorhombic spectrum of Fe^{3+} confirms the peculiar capability of iron ions to substitute for both K^+ and Ta^{5+} ions, thereby producing both axial and orthorhombic paramagnetic centers.

Finally, manganese impurities, apparently related to the sample growing method, are detected by light excitation. Their charge state in nominally pure potassium tantalate seems to depend on the presence of other impurities.

ACKNOWLEDGMENTS

The authors gratefully acknowledge Professor P. Camagni and Professor G. Samoggia for their interesting and helpful discussions and A. Slipenjuk and L. Bolis for assistance in calculations.

[1]D. Rytz, A. Châtelain, and U. T. Höchli, Phys. Rev. B **27**, 6830 (1983).
[2]B. E. Vugmeister and M. D. Glinchuk, Rev. Mod. Phys. **82**, 993 (1990).
[3]Y. Yacobi, A. Agranat, and I. Ohana, Solid State Commun. **45**, 757 (1983).
[4]U. T. Höchli, H. E. Weibel, and L. A. Boatner, J. Phys. C **12**, L562 (1979).
[5]W. Kleemann, S. Kutz, F. J. Shafer, and D. Rytz, Phys. Rev. B **37**, 5856 (1988).
[6]W. Kleeman, F. J. Shafer, and D. Rytz, Phys. Rev. Lett. **54**, 2038 (1985).
[7]M. Stachiotti, A. Dobry, R. Migoni, and A. Bussmann-Holder, Phys. Rev. B **47**, 2473 (1993).
[8]M. D. Glinchuk and V. A. Stephanovich, J. Phys. Condens. Matter (to be published).
[9]Y. Yacobi, Z. Phys. B **31**, 275 (1978).
[10]H. Uwe, K. B. Lyons, H. L. Carter, and P. A. Fleury, Phys. Rev. B **33**, 6436 (1986).
[11]S. Jandl, P. Grenier, and L. A. Boatner, Ferroelectrics **107**, 73 (1990).
[12]H. Vogt, Phys. Rev. B **41**, 1184 (1990); J. Phys. Condens. Matter **3**, 3697 (1991).
[13]P. Grenier, G. Bernier, S. Jandl, and L. A. Boatner, J. Phys. Condens. Matter **1**, 2515 (1989).
[14]E. Yamaichi, K. Watanabe, and K. Ohi, J. Phys. Soc. Jpn. **57**, 2201 (1988).
[15]E. Yamaichi, S. Ohno, and K. Ohi, Jpn. J. Appl. Phys. **27**, 583 (1988).
[16]R. S. Klein, G. E. Kugel, M. D. Fontana, and U. T. Höchli, Ferroelectrics **125**, 325 (1992).
[17]R. S. Klein, G. E. Kugel, M. D. Glinchuk, R. O. Kuzian, and I. V. Kondakova (private communication).
[18]S. A. Altshuler and V. M. Kozyrev, *Electron Paramagnetic*

Resonance (Nauka, Moscow, 1972).
[19]A. P. Pechenyi, M. D. Glinchuk, T. V. Antimirova, and W. Kleemann, Phys. Status Solidi B **174**, 325 (1992).
[20]D. M. Hannon, Phys. Rev. B **3**, 2153 (1971).
[21]D. M. Hannon, Phys. Rev. B **164**, 366 (1967).
[22]I. P. Bykov, M. D. Glinchuk, A. A. Karmazin, and V. V. Laguta, Fiz. Tverd. Tela (Leningrad) **25**, 3586 (1983) [Sov. Phys. Solid State **25**, 2063 (1983)].
[23]R. Berny, D. Cowan, and F. Morin, Solid State Commun. **26**, 579 (1978).
[24]E. Possenriede, P. Jacobs, and O. F. Schirmer, J. Phys. Condens. Matter **4**, 4719 (1992), and references therein.
[25]M. M. Abragam, L. A. Boatner, D. N. Olson, and U. T. Höchli, J. Chem. Phys. **81**, 2528 (1984).
[26]I. Laulicht, Y. Yacobi, and A. Baram, J. Chem. Phys. **91**, 79 (1989).
[27]I. P. Bykov, I. N. Geifman, M. D. Glinchuk, and B. K. Krulikovskii, Sov. Phys. Solid State **22**, 1248 (1980).
[28]E. Siegel and K. A. Müller, Phys. Rev. B **19**, 109 (1979).
[29]R. A. Serway, W. Berlinger, K. A. Müller, and R. W. Collins, Phys. Rev. B **16**, 4761 (1977).